

Supporting information

Self-assembly of silver (I)
metallomacrocycles using unsupported 1,4-
substituted-1,2,3-triazole “Click” ligands.

*Martin L.Gower and James D Crowley**

Department of Chemistry, University of Otago, PO Box 56, Dunedin, New Zealand

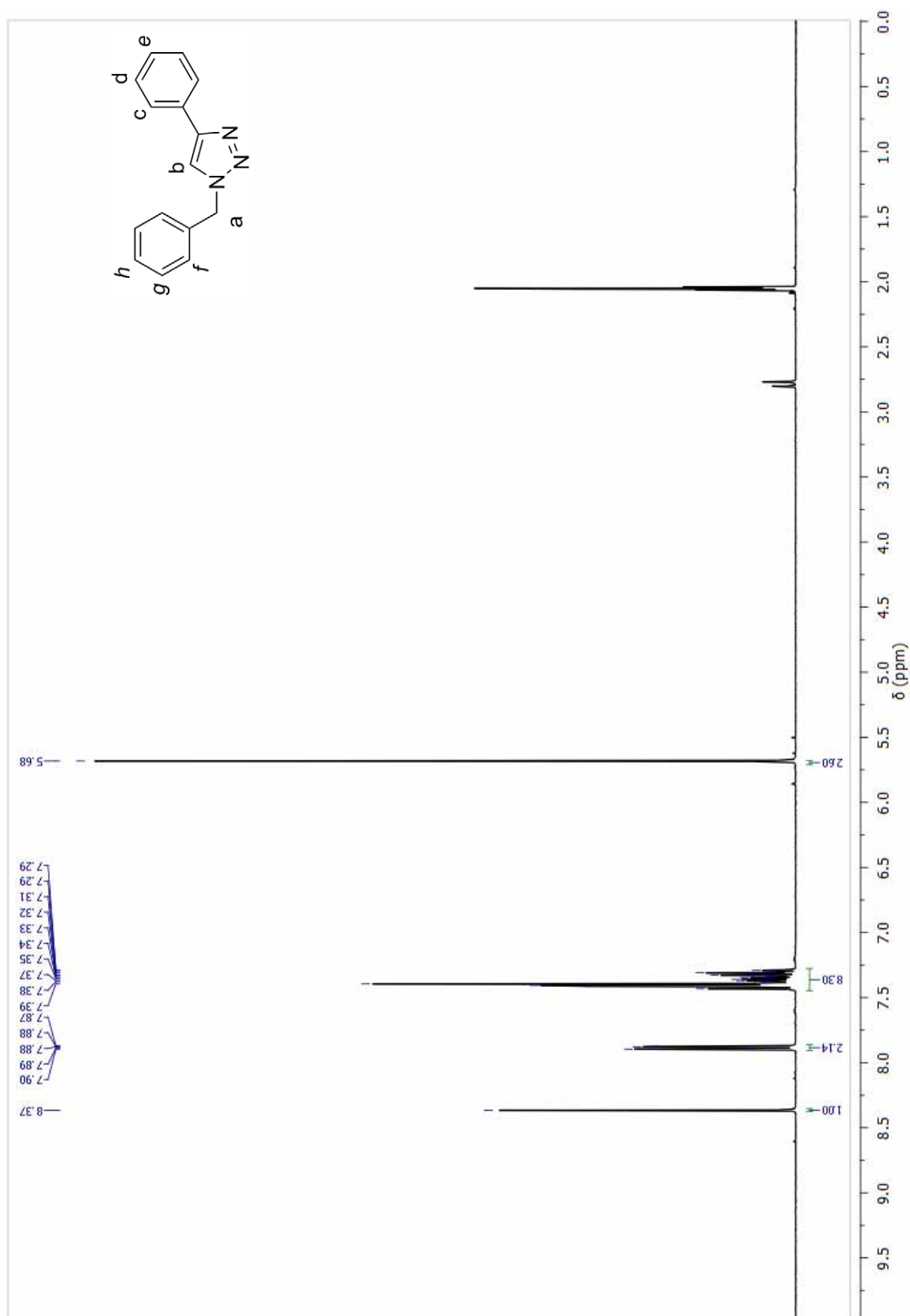
jcrowley@chemistry.otago.ac.nz

Table of Contents	S2
1. ¹H NMR Spectra of synthesized compounds.	S4
¹ H NMR (<i>d</i> ₆ -acetone, 300K) of 2a .	S4
¹ H NMR (<i>d</i> ₆ -acetone, 300K) of 2b .	S5
¹ H NMR (<i>d</i> ₆ -acetone, 300K) of 3a .	S6
¹ H NMR (<i>d</i> ₆ -acetone, 300K) of 3b .	S7
¹ H NMR (<i>d</i> ₆ -acetone, 300K) of 4a .	S8
Figure 1. Partial ¹ H NMR spectra (300 MHz, <i>d</i> ₆ -acetone, 300 K) of a) Ligand 2a , b) [Ag ₂ (2a) ₂](SbF ₆) ₂ , 4a .	S8
¹ H NMR (<i>d</i> ₆ -acetone, 300K) of 4b .	S9
Figure 2. Partial ¹ H NMR spectra (300 MHz, <i>d</i> ₆ -acetone, 300 K) of a) Ligand 2b , b) [Ag ₂ (2b) ₂](SbF ₆) ₂ .	S9
¹ H NMR (<i>d</i> ₆ -acetone, 300K) of 5a .	S10
Figure 3. Partial ¹ H NMR spectra (300 MHz, <i>d</i> ₆ -acetone, 300 K) of a) Ligand 3a , b) [Ag ₂ (3a) ₂](SbF ₆) ₂ , 5a .	S10
¹ H NMR (<i>d</i> ₆ -acetone, 300K) of [Ag ₂ (5b) ₂](SbF ₆) ₂ .	S11
Figure 4. Partial ¹ H NMR spectra (300 MHz, <i>d</i> ₆ -acetone, 300 K) of a) Ligand 3b , b) [Ag ₂ (3b) ₂](SbF ₆) ₂ , 5b .	S11
2. SPARTAN CPK models of the silver(I) complexes.	S12
Figure 5. Space Filling (CPK, left) and tube (right) molecular models of the trimeric 3:3 complex formed between 2a and Ag(SbF ₆).	S12
Figure 6. Space Filling (CPK, left) and tube (right) molecular models showing the complex formed if Ag(I) binding to the ligands (3a and 3b) was through the N2 nitrogen of the triazole.	S12

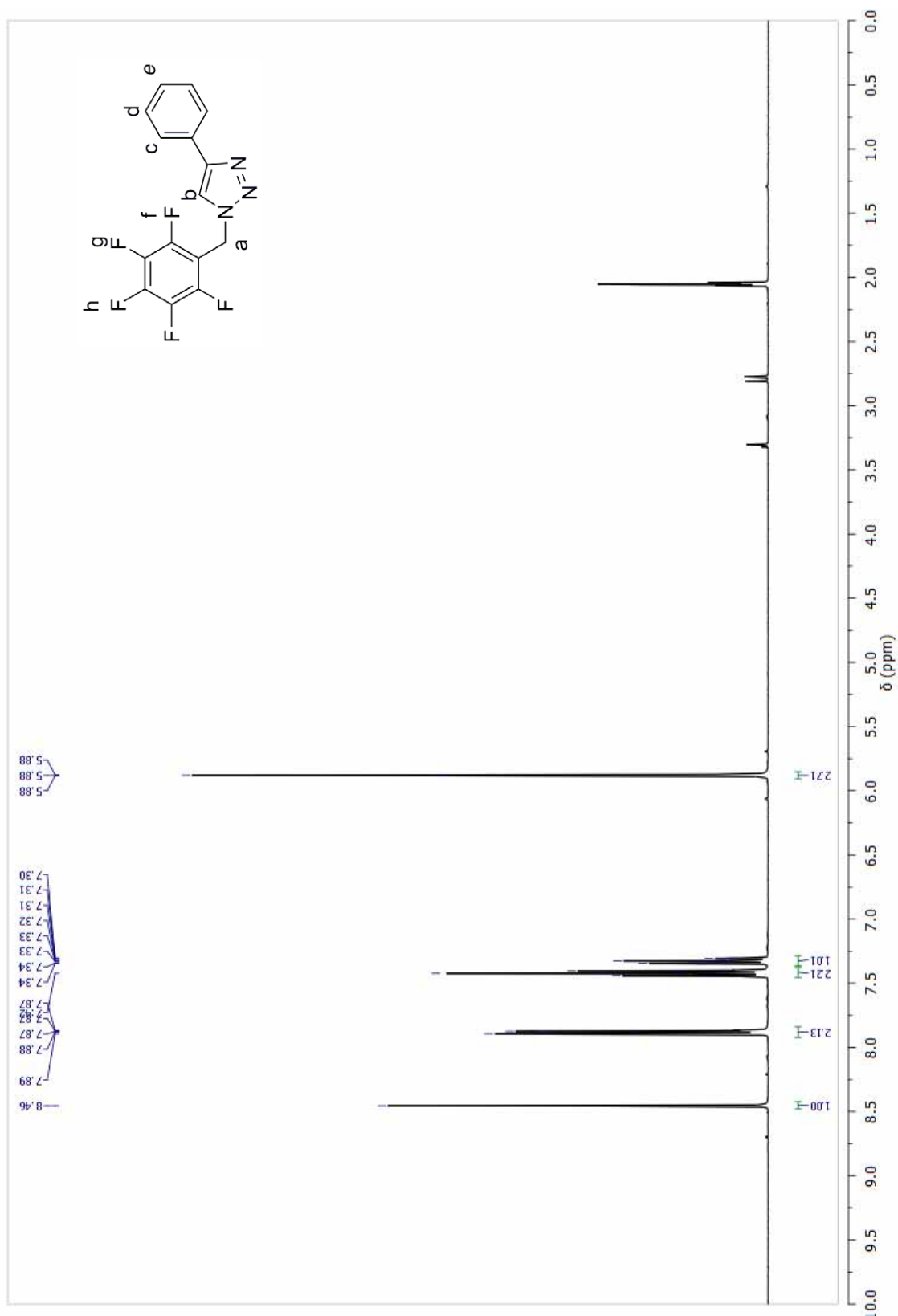
3. HR-ESMS Spectra of the silver complexes.	S13
Figure 7. HR-ESMS (CH ₃ CN) of [Ag ₂ (2a) ₂](SbF ₆) ₂ , 4a .	S13
Figure 8. Observed and Calculated isotopic distributions for the [Ag ₂ (2a) ₂](SbF ₆) ⁺ ion.	S14
Figure 9. HR-ESMS (CH ₃ CN) of [Ag ₂ (2b) ₂](SbF ₆) ₂ , 4b .	S15
Figure 10. Observed and Calculated isotopic distributions for the [Ag ₂ (2b) ₂](SbF ₆) ₂ ⁺ ion.	S16
Figure 11. HR-ESMS (CH ₃ CN) of [Ag ₂ (3a) ₂](SbF ₆) ₂ , 5a .	S17
Figure 12. Observed and Calculated isotopic distributions for the [Ag ₂ (3a) ₂](SbF ₆) ₂ ⁺ ion.	S18
Figure 13. HR-ESMS (CH ₃ CN) of [Ag ₂ (3b) ₂](SbF ₆) ₂ , 5b .	S19
Figure 15. Observed and Calculated isotopic distributions for the [Ag ₂ (3b) ₂](SbF ₆) ₂ ⁺ ion.	S20
4. X-ray Crystallographic Data	S21
Figure 15. ORTEP (top) and space filling (bottom) views of the [2 a ₂ Ag ₂] ²⁺ cation.	S21
Figure 16. Two views of [(2a) ₂ Ag ₂](SbF ₆) ₂ (3a) showing the close contacts between the SbF ₆ ⁻ anions and the Ag(I) ions.	S22
Figure 17. Two views of the extended structure of [(2a) ₂ Ag ₂](SbF ₆) ₂ (3a). a) a ball and stick diagram and b) a space filing diagram.	S22
Figure 18. ORTEP (top) and space filling (bottom) views of the [(2b) ₄ Ag ₂] ²⁺ cation.	S23
Figure 19. Two views of the extended structure of [(2b) ₂ Ag ₂](SbF ₆) ₂ (3b). a) a ball and stick diagram and b) a space filing diagram.	S24
Figure 20. An ORTEP diagram of the [(3b) ₄ Ag ₂] ²⁺ cation.	S24
Figure 21. Two views of the complete cationic unit of [(3b) ₂ Ag ₂](SbF ₆) ₂ (5b). a) a ball and stick diagram and b) a space filing diagram.	S25
Figure 22. Two views of the extended structure of [(3b) ₂ Ag ₂](SbF ₆) ₂ (5b). a) a ball and stick diagram and b) a space filing diagram.	S25
4.1 X-Ray data collection and refinement for 5b (acetone).	S26
Table 1 Crystal data and structure refinement for 5b (acetone).	S26
Figure 23. An ORTEP diagram of [(3b) ₄ Ag ₂] ²⁺ cation from the of the crystal structure 5b (acetone)	S27
5. References.	S27

1. ^1H NMR spectra of synthesized compounds.

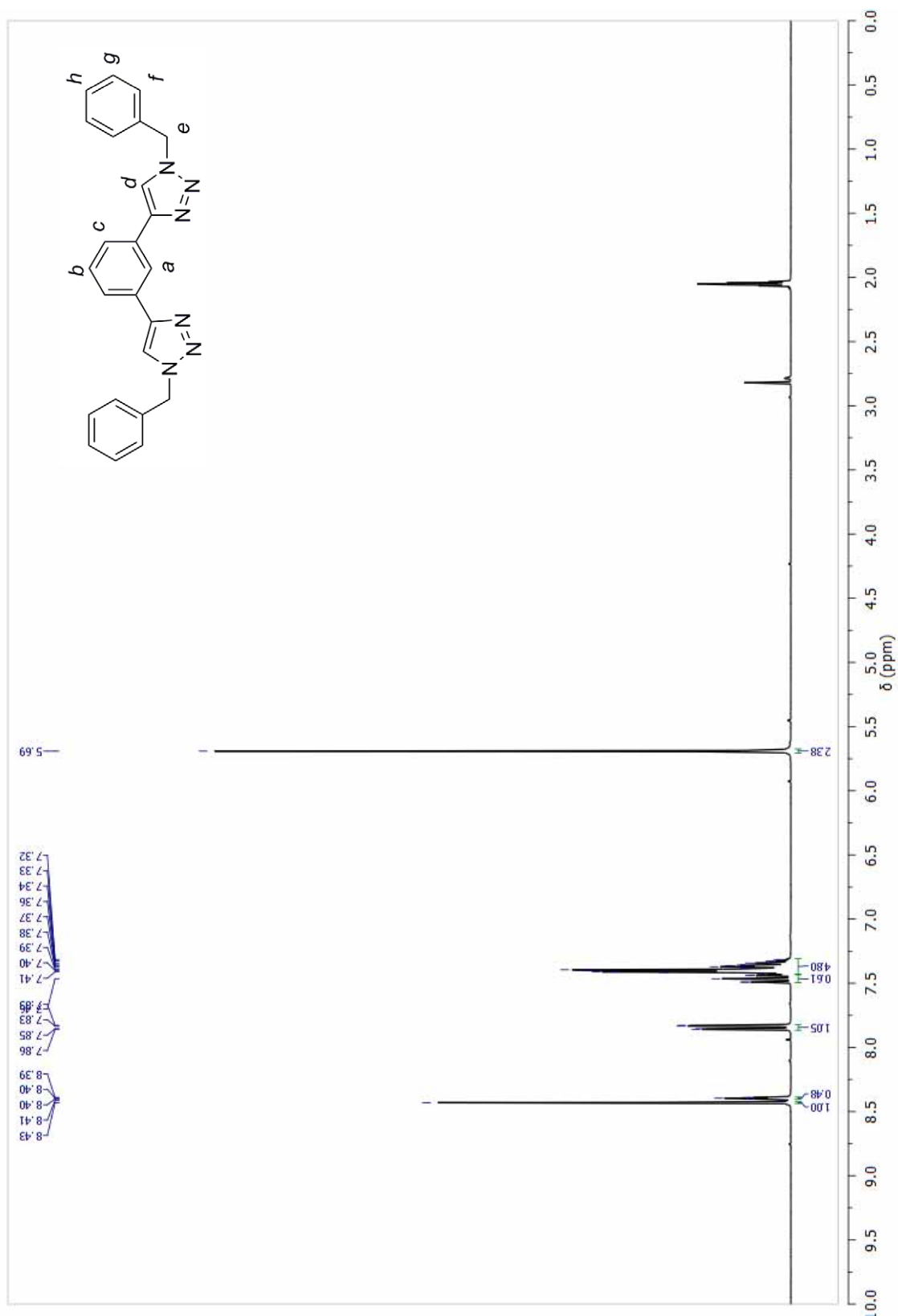
^1H NMR (d_6 -acetone, 300K) of **2a**.



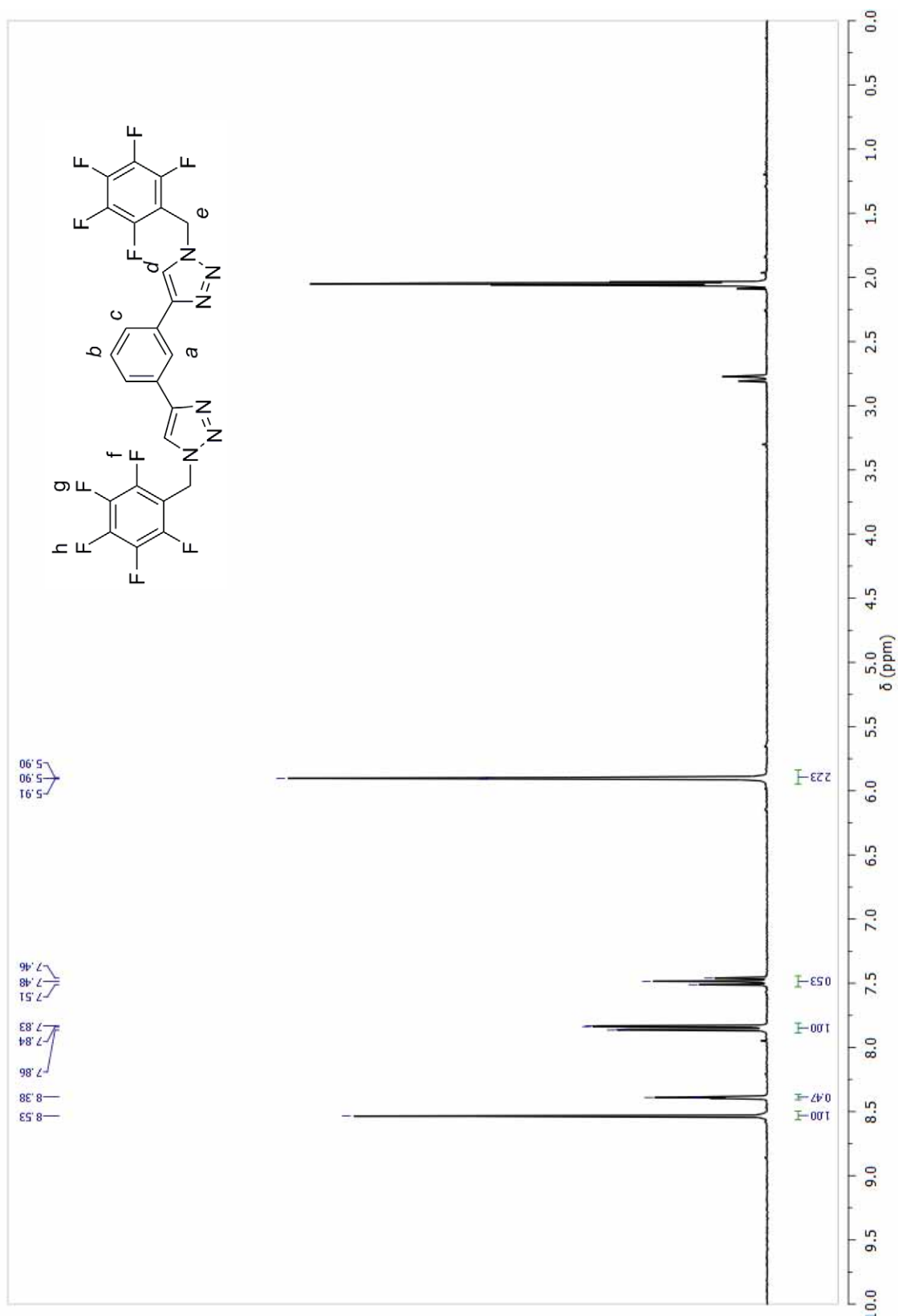
^1H NMR (d_6 -acetone, 300K) of **2b**.



^1H NMR (d_6 -acetone, 300K) of **3a**.



^1H NMR (d_6 -acetone, 300K) of **3b**.



4.1 ^1H NMR spectra of the silver(I) complexes.

^1H NMR (d_6 -acetone, 300K) of **4a**.

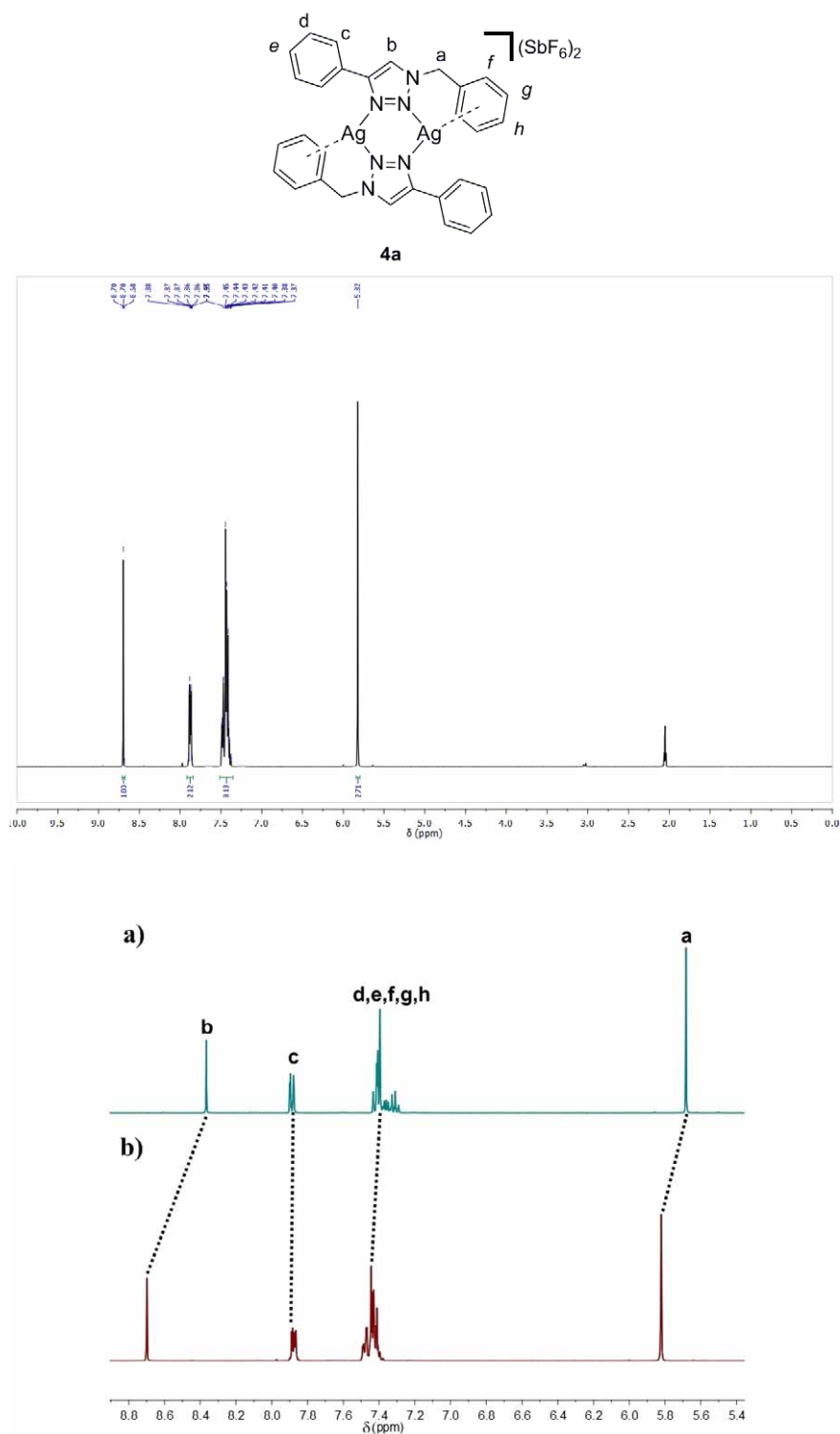


Figure 1. Partial ^1H NMR spectra (300 MHz, d_6 -acetone, 300 K) of a) Ligand **2a**, b) silver complex **4a**.

^1H NMR (d_6 -acetone, 300K) of **4b**.

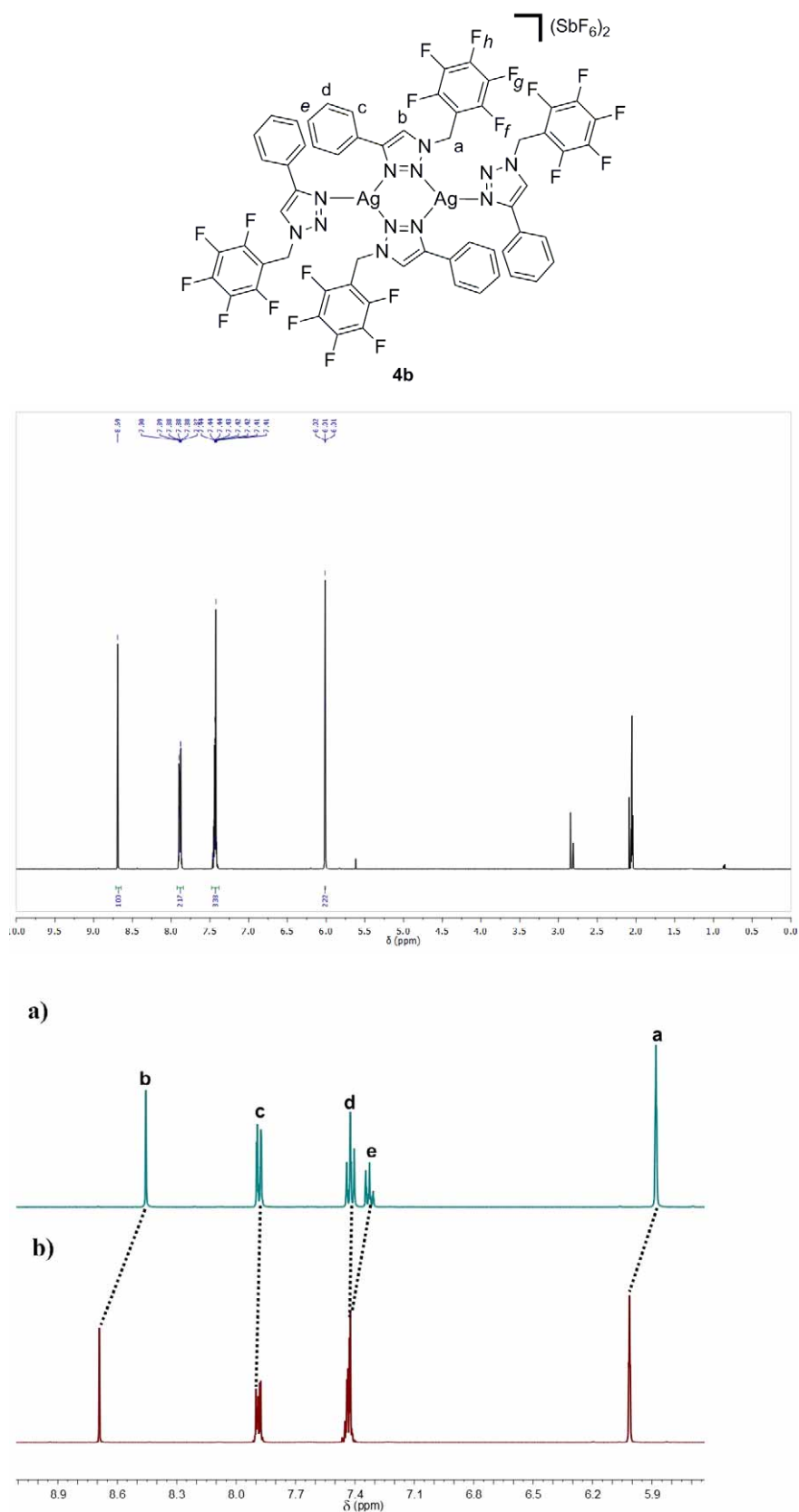


Figure 2. Partial ^1H NMR spectra (300 MHz, d_6 -acetone, 300 K) of a) Ligand **2b**, b) silver complex **4b**.

^1H NMR (d_6 -acetone, 300K) of **5a**.

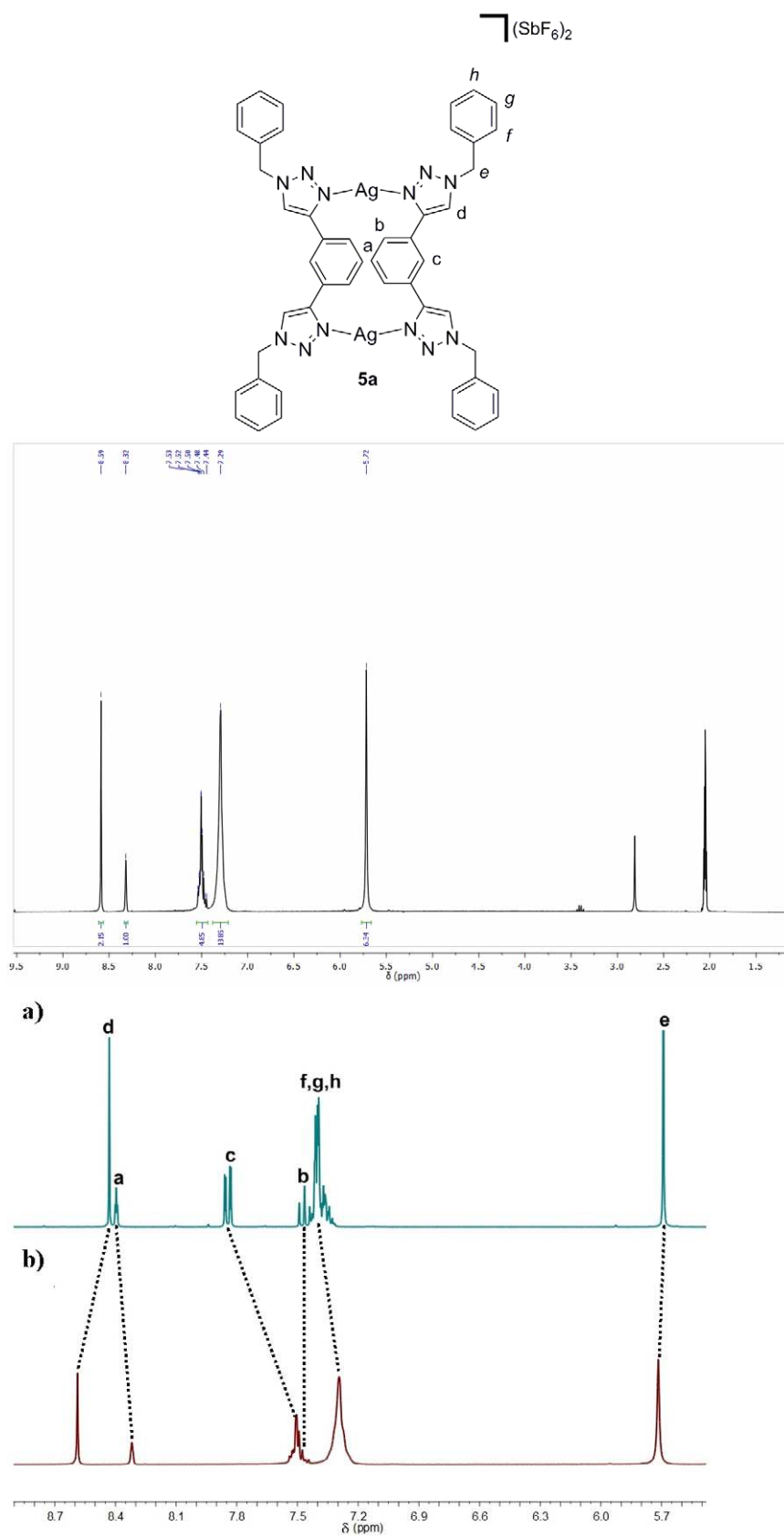


Figure 3. Partial ^1H NMR spectra (300 MHz, d_6 -acetone, 300 K) of a) Ligand **3a**, b) silver complex **5a**.

^1H NMR (d_6 -acetone, 300K) of **5b**.

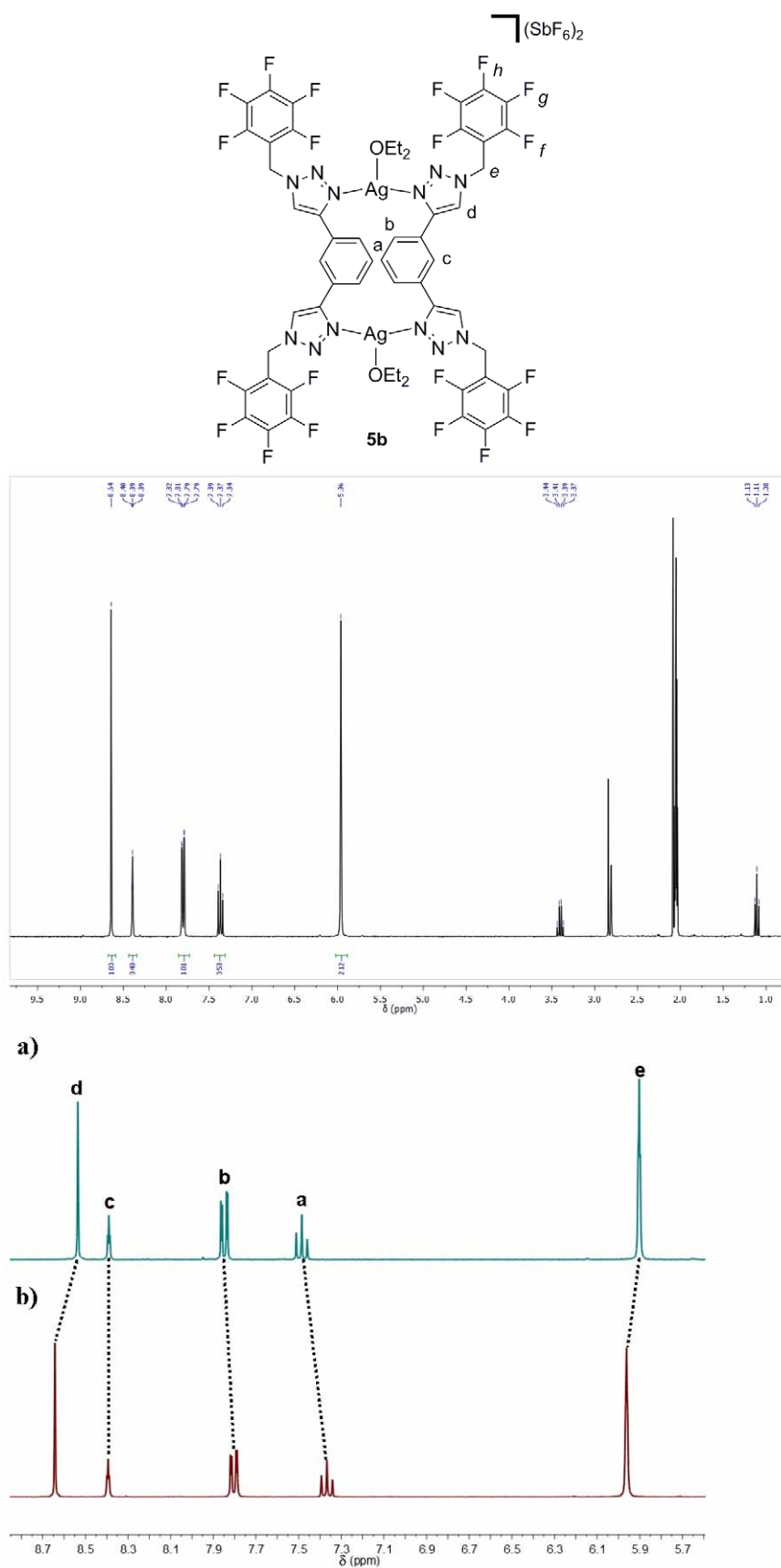


Figure 4. Partial ^1H NMR spectra (300 MHz, d_6 -acetone, 300 K) of a) Ligand **3b**, b) **5b**.

2. SPARTAN CPK molecular models of the complexes.

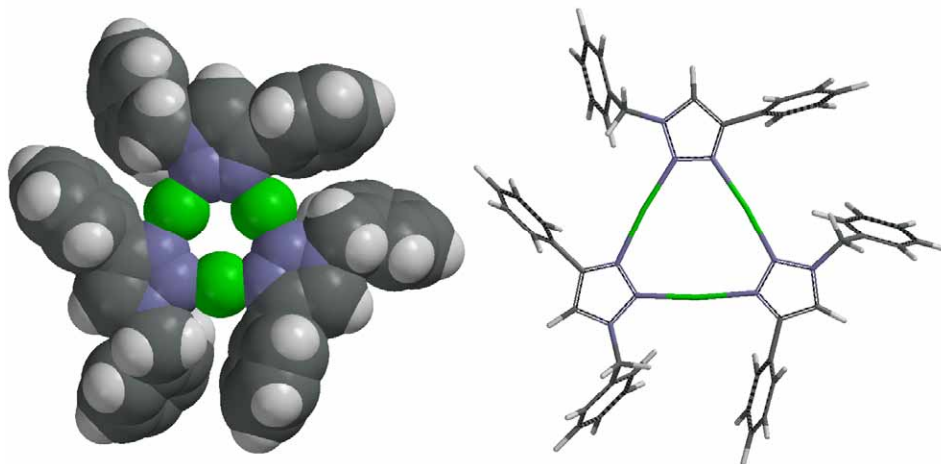


Figure 5. Space Filling (CPK, left) and tube (right) molecular models of the trimeric 3:3 complex formed between **2a** and Ag(SbF₆). (Spartan '06 Essential Edition for Windows, Wavefunction, Irvine, CA)

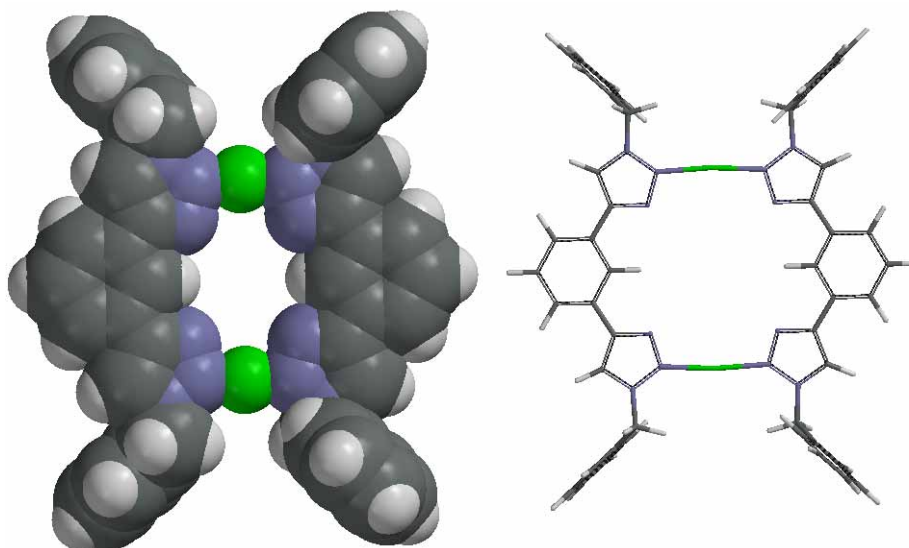


Figure 6. Space Filling (CPK, left) and tube (right) molecular models showing the complex formed if Ag(I) binding to the ligands (**3a** and **3b**) was through the N2 nitrogen of the triazole. (Spartan '06 Essential Edition for Windows, Wavefunction, Irvine, CA)

3. HR-ESMS spectra of the silver(I) complexes.

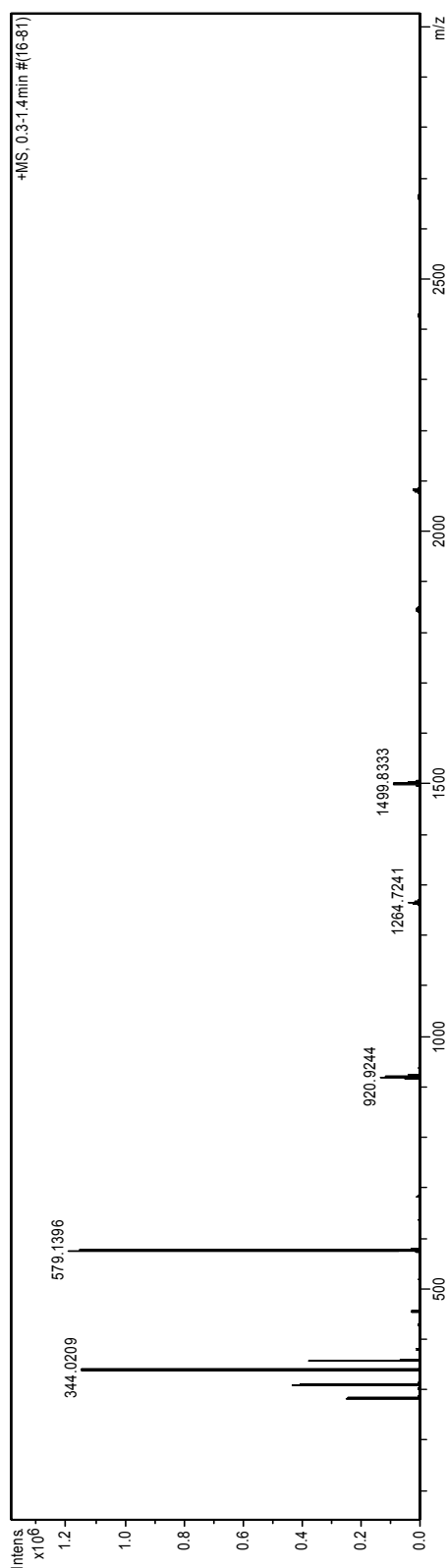


Figure 7. HR-ESMS (CH_3CN) of $[\text{Ag}_2(\mathbf{2a})_2](\text{SbF}_6)_2$, **4a**: $m/z = 344.0209$ $[\text{Ag}(\mathbf{2a})]^+$ (calc. for $\text{C}_{15}\text{H}_{13}\text{AgN}_3$ 344.0157), 579.1396 $[\text{Ag}(\mathbf{2a})_2]^+$ (calc. for $\text{C}_{30}\text{H}_{26}\text{AgN}_6$ 579.1267), 920.9243 $[\text{Ag}_2(\mathbf{2a})_2](\text{SbF}_6)^+$ (calc. for $\text{C}_{30}\text{H}_{26}\text{Ag}_2\text{F}_6\text{N}_6\text{Sb}$ 920.9245), 1499.8332 $[\text{Ag}_3(\mathbf{2a})_3](\text{SbF}_6)_2^+$ (calc. for

$C_{45}H_{39}Ag_3F_{12}N_9Sb_2$ 1499.8367).

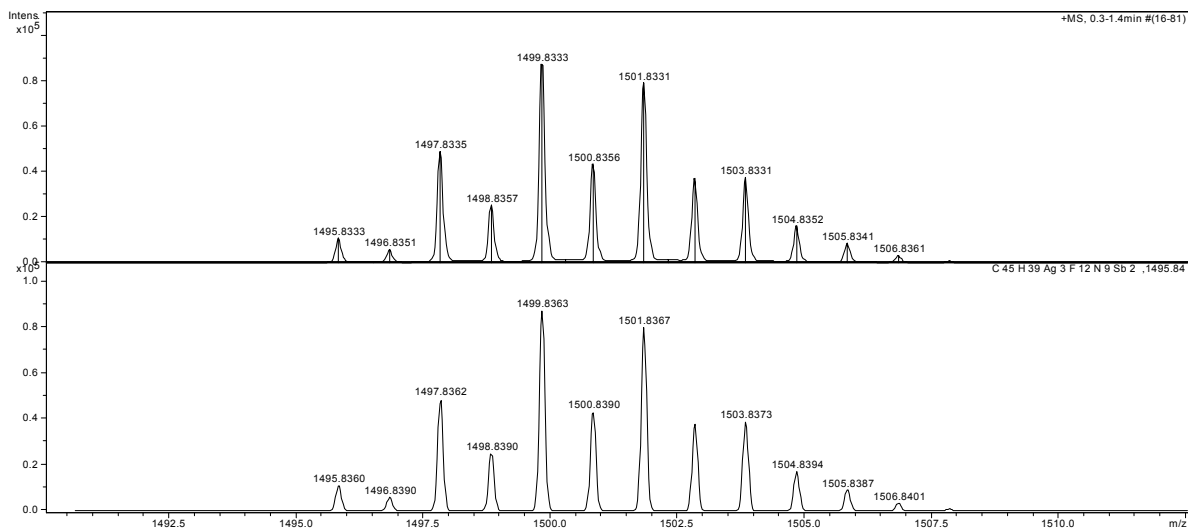


Figure 8. Observed (top) and calculated (bottom) isotopic distribution for the $[Ag_3(2a)_3](SbF_6)_2^+$ ion.

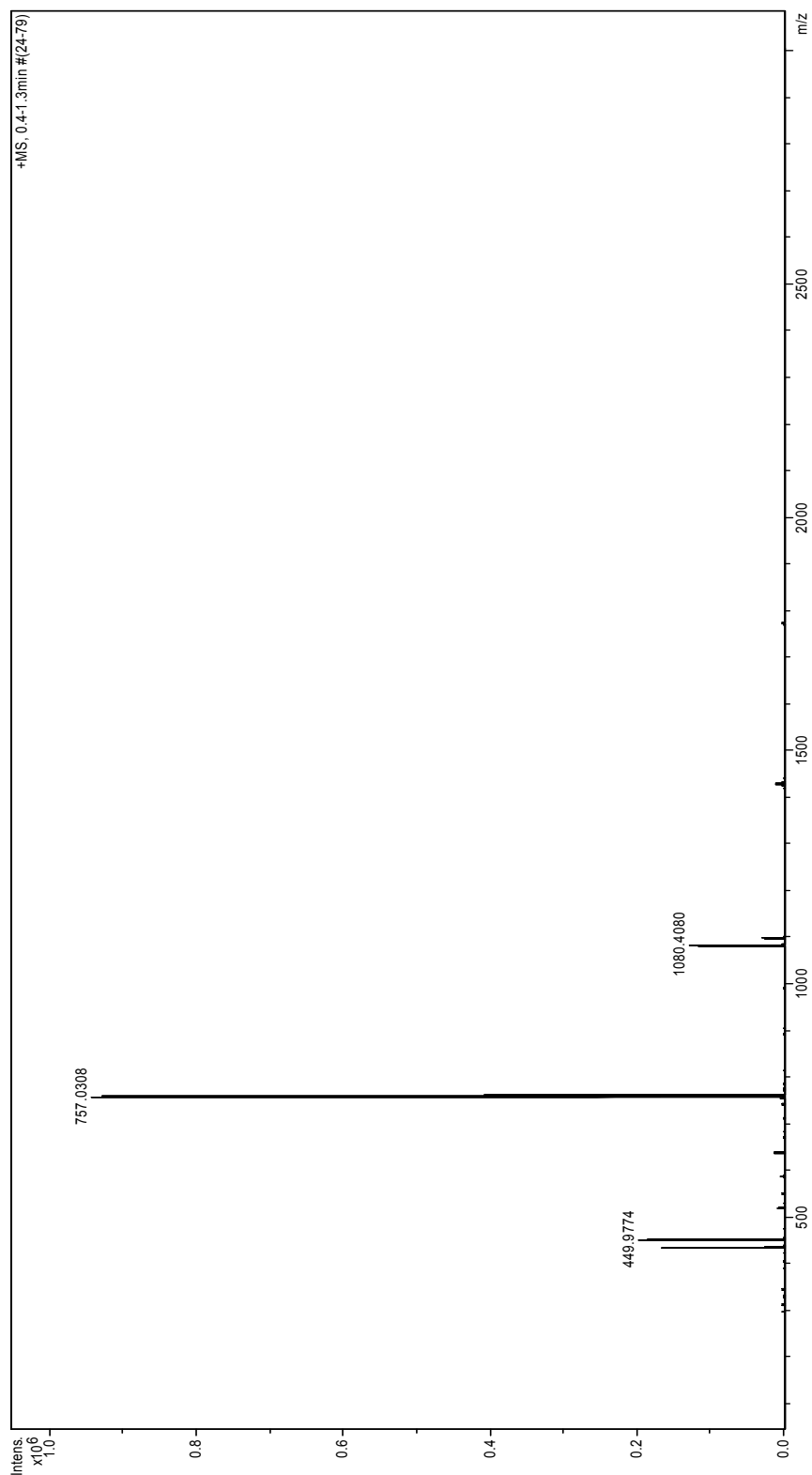


Figure 9. HR-ESMS (CH₃CN) of [Ag₂(**2b**)₂](SbF₆)₂, **4b**: $m/z = 449.9775$ [Ag(**2b**)H₂O]⁺ (calc. for C₁₅H₁₀AgF₅N₃O 449.9795), 757.0273 [Ag(**2b**)₂]⁺ (calc. for C₃₀H₁₆AgF₁₀N₆ 757.0328), 1425.8874 [Ag₂(**2b**)₃](SbF₆)⁺ (calc. for C₄₅H₂₄Ag₂F₂₁N₉Sb 1425.8960), 1769.6885 [Ag₃(**2b**)₃](SbF₆)⁺ (calc. for

C₄₅H₂₄Ag₃F₂₇N₉Sb₂ 1769.6953).

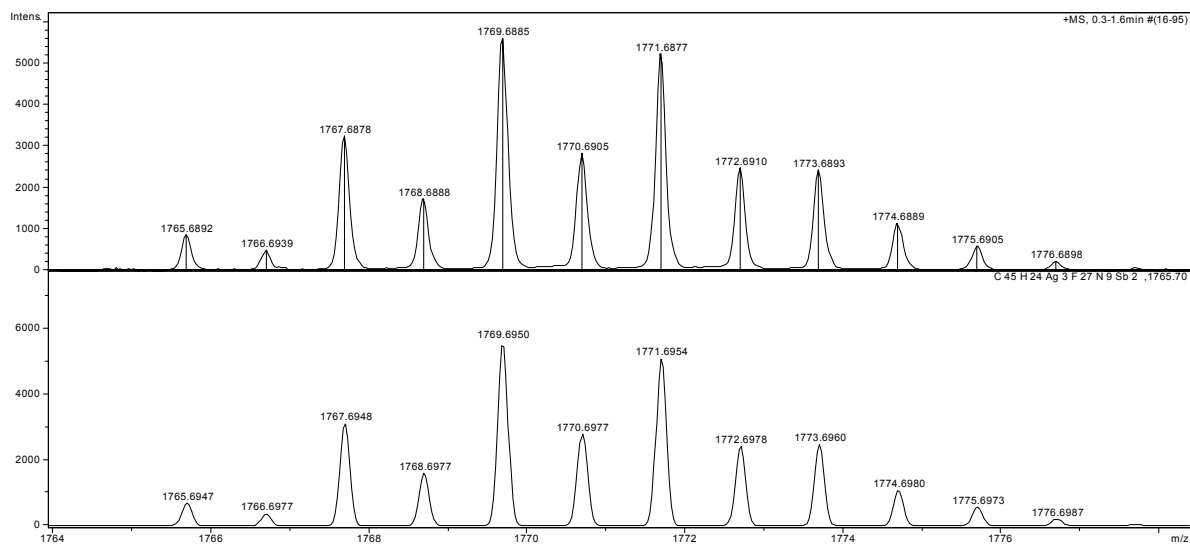


Figure 10. Observed (top) and calculated (bottom) isotopic distribution for the [Ag₃(**2b**)₃](SbF₆)₂⁺ ion.

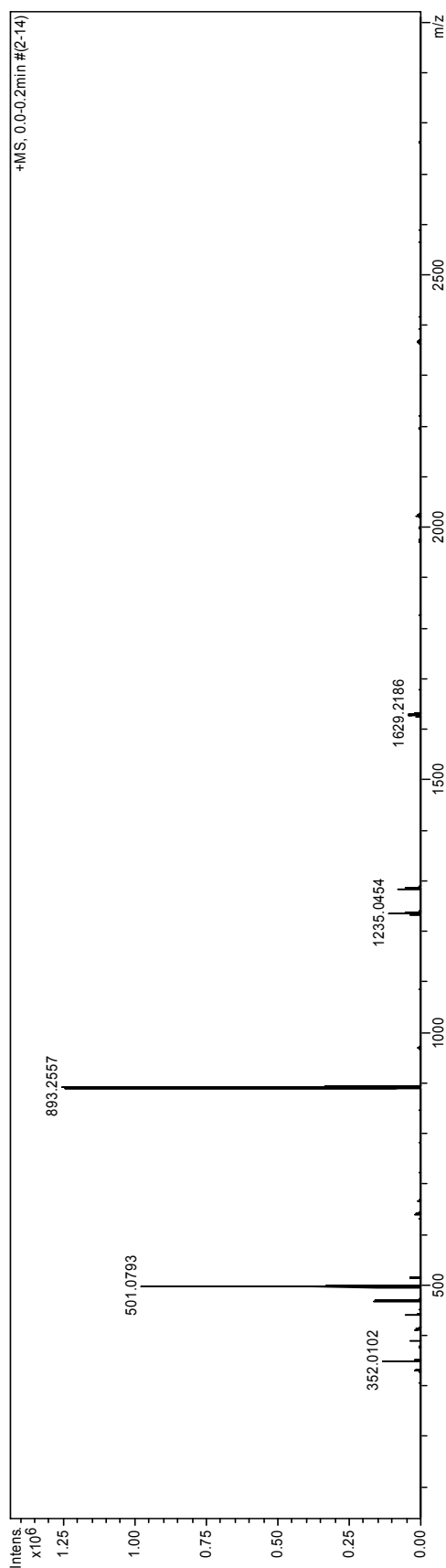


Figure 11. HR-ESMS (CH_3CN) of $[\text{Ag}_2(\mathbf{3a})_2](\text{SbF}_6)_2$, **5a**: $m/z = 501.0789$ $[\text{Ag}(\mathbf{3a})]^+$ (calc. for $\text{C}_{24}\text{H}_{20}\text{N}_6\text{Ag}$ 501.0797), 893.2551 $[\text{Ag}(\mathbf{3a})_2]^+$ (calc. for $\text{C}_{48}\text{H}_{40}\text{AgN}_6$ 893.2543), 1235.0454

$[\text{Ag}_2(\mathbf{3a})_2](\text{SbF}_6)^+$ (calc. for $\text{C}_{48}\text{H}_{40}\text{N}_{12}\text{Ag}_2\text{SbF}_6$ 1235.0540), 1629.2186 $[\text{Ag}_2(\mathbf{3a})_3](\text{SbF}_6)^+$ (calc. for $\text{C}_{72}\text{H}_{60}\text{N}_{18}\text{Ag}_2\text{SbF}_6$ 1629.2293).

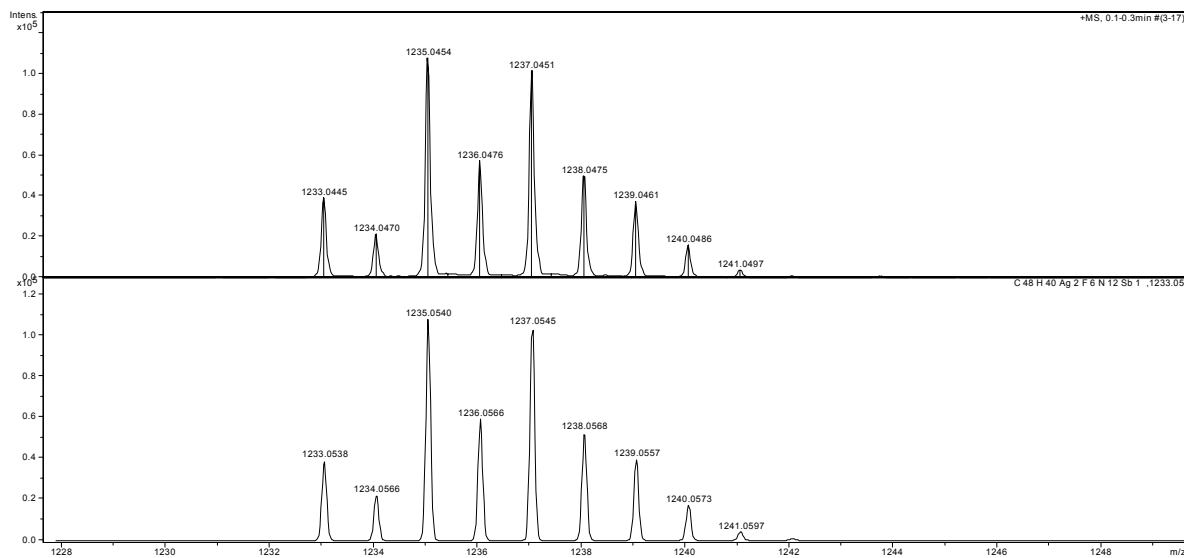


Figure 12. Observed (top) and calculated (bottom) isotopic distribution for the $[\text{Ag}_2(\mathbf{3a})_2](\text{SbF}_6)^+$ ion.

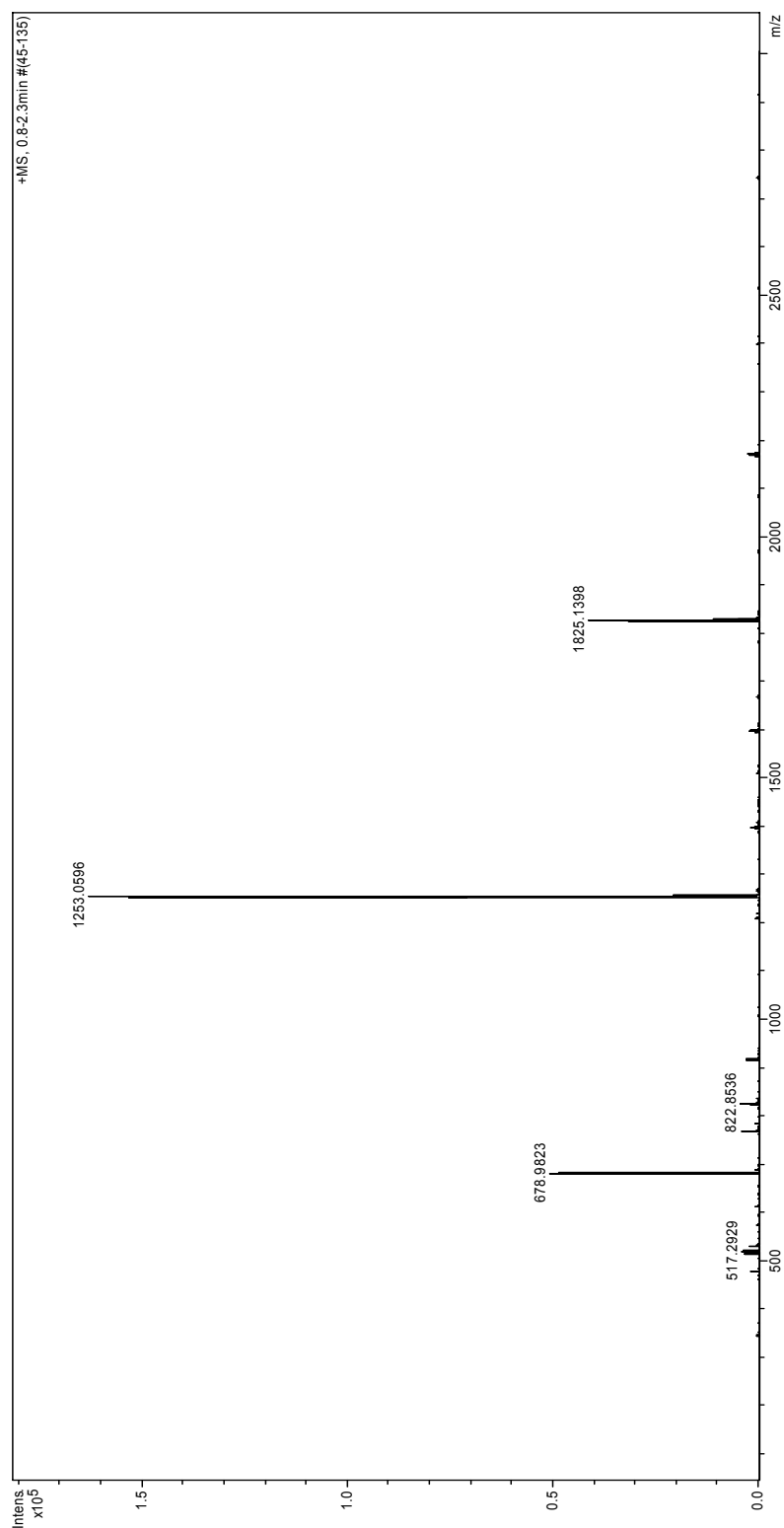


Figure 13. HR-ESMS (CH_3CN) of $[\text{Ag}_2(\mathbf{3b})_2](\text{SbF}_6)_2$, **5b**: $m/z = 678.9967$ $[\text{Ag}(\mathbf{3b})]^+$ (calc. for $\text{C}_{24}\text{H}_{10}\text{AgF}_{10}\text{N}_6$ 678.9858), 1253.0809 $[\text{Ag}(\mathbf{3b})_2]^+$ (calc. for $\text{C}_{48}\text{H}_{20}\text{AgF}_{20}\text{N}_{12}$ 1253.0662), 1594.8573

$[\text{Ag}_2(\mathbf{3b})_2](\text{SbF}_6)^+$ (calc. for $\text{C}_{48}\text{H}_{20}\text{Ag}_2\text{F}_{26}\text{N}_{12}\text{Sb}$ 1594.8655), 1825.1623 $[\text{Ag}(\mathbf{3b})_3]^+$ (calc. for $\text{C}_{72}\text{H}_{30}\text{AgF}_{30}\text{N}_{18}$ 1825.1469).

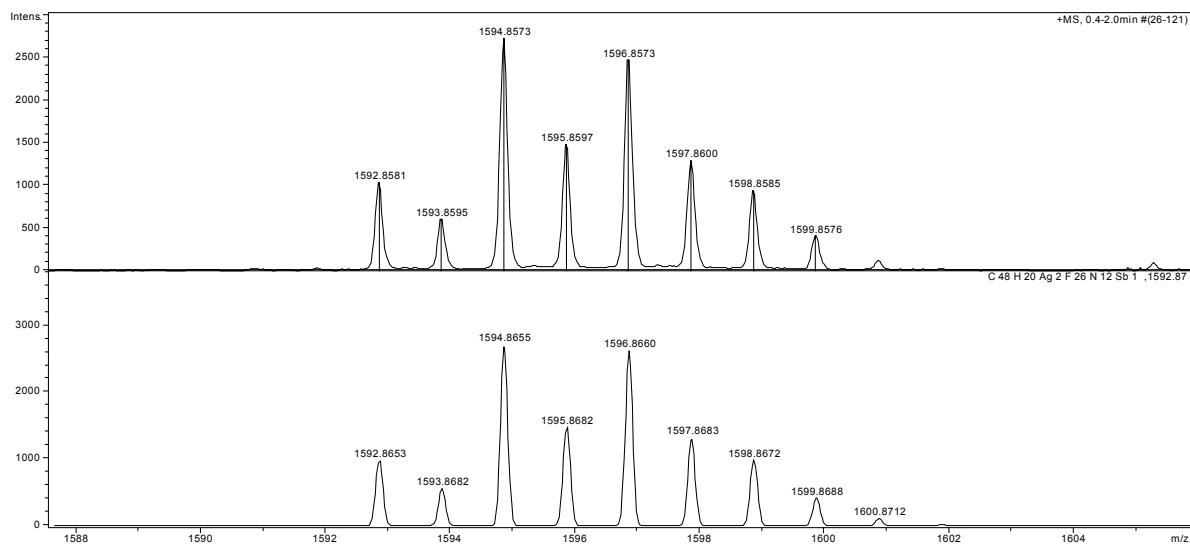


Figure 14. Observed (top) and calculated (bottom) isotopic distribution for the $[\text{Ag}_2(\mathbf{3b})_2](\text{SbF}_6)^+$ ion.

7. X-ray data for the silver (I) complexes.

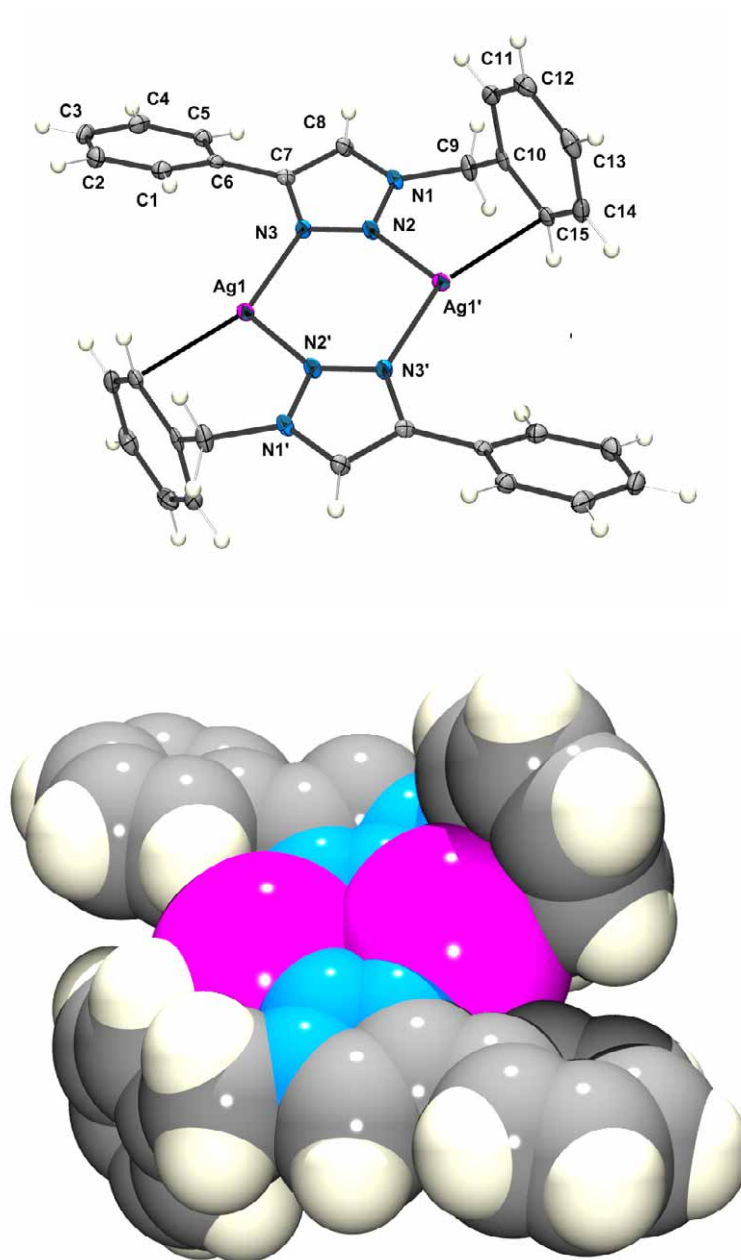


Figure 15. ORTEP (top) and space filling (bottom) views of the $[(2a)_2Ag_2]^{2+}$ cation. The SbF_6^- anions are omitted for clarity.

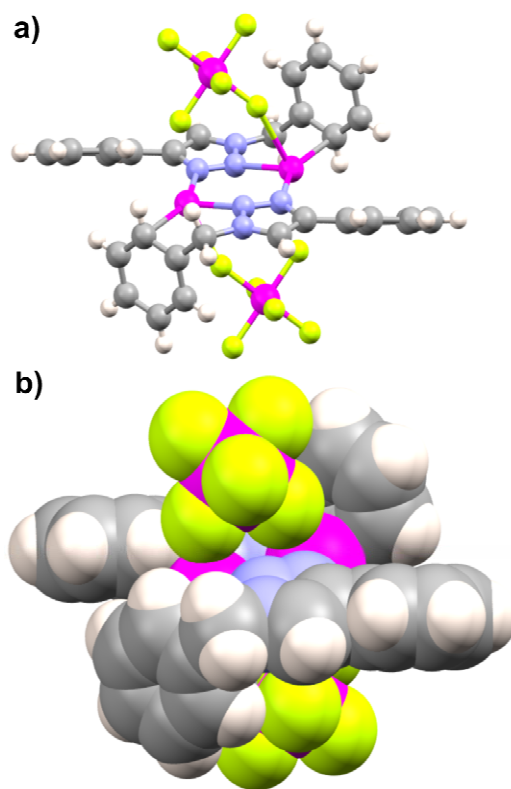


Figure 16. Two views of $[(2\mathbf{a})_2\text{Ag}_2](\text{SbF}_6)_2$ ($\mathbf{3a}$) showing the close contacts between the SbF_6^- anions and the Ag(I) ions. a) a ball and stick diagram and b) a space filing diagram.

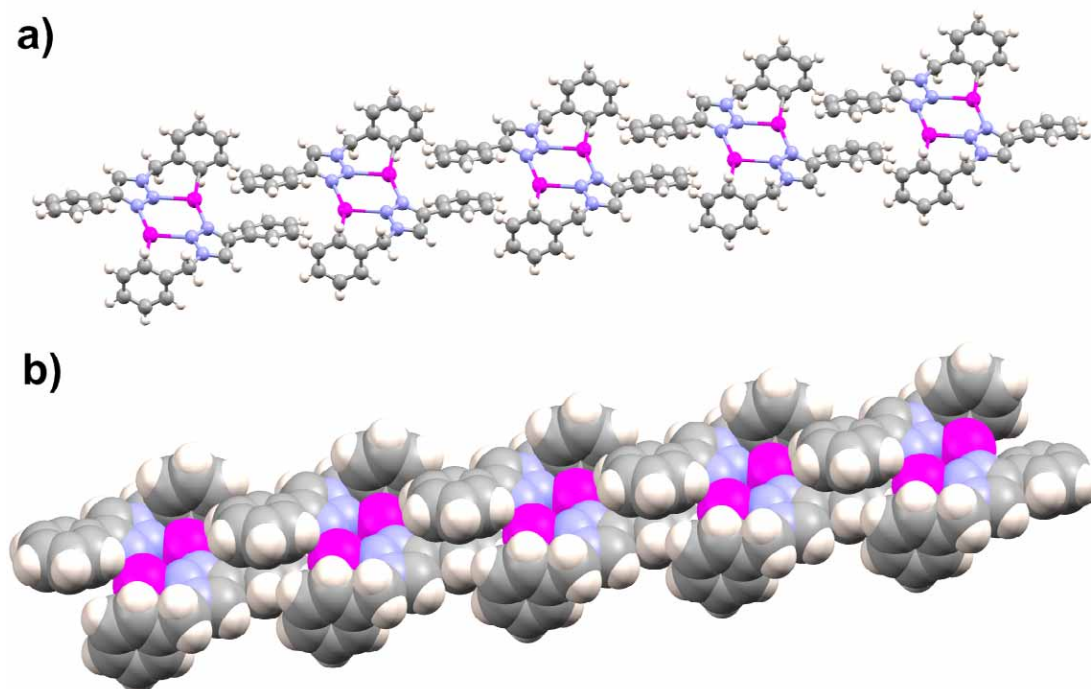


Figure 17. Two views of the extended structure of $[(2\mathbf{a})_2\text{Ag}_2](\text{SbF}_6)_2$ ($\mathbf{3a}$). a) a ball and stick diagram and b) a space filing diagram. The SbF_6^- anions are omitted for clarity.

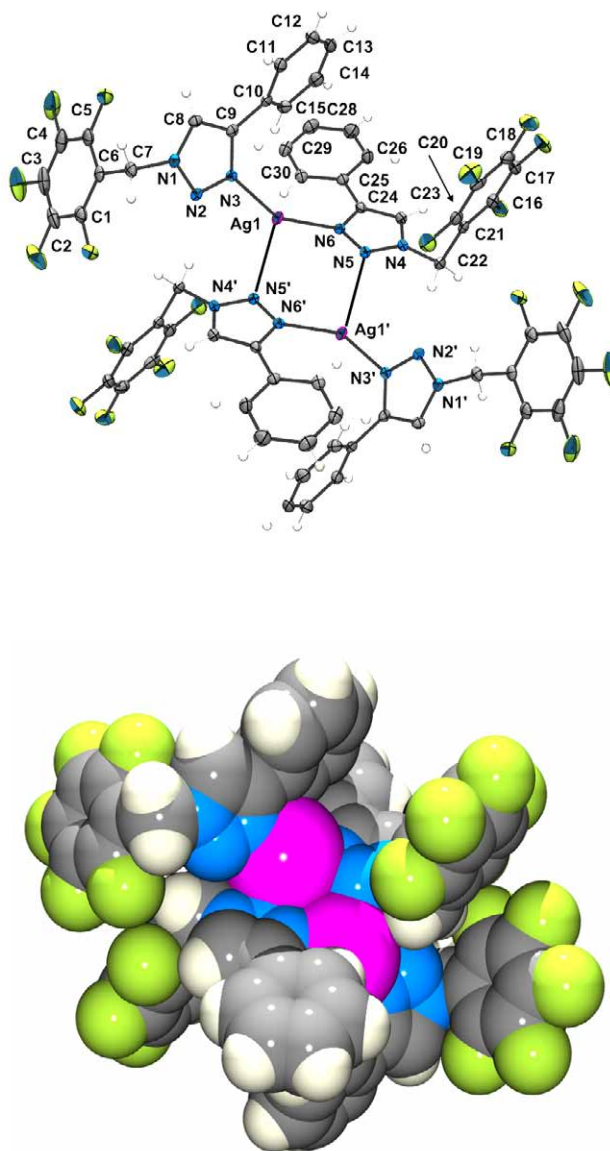


Figure 18. ORTEP (top) and space filling (bottom) views of the $[(2b)_4Ag_2]^{2+}$ cation. The SbF_6^- anions are omitted for clarity.

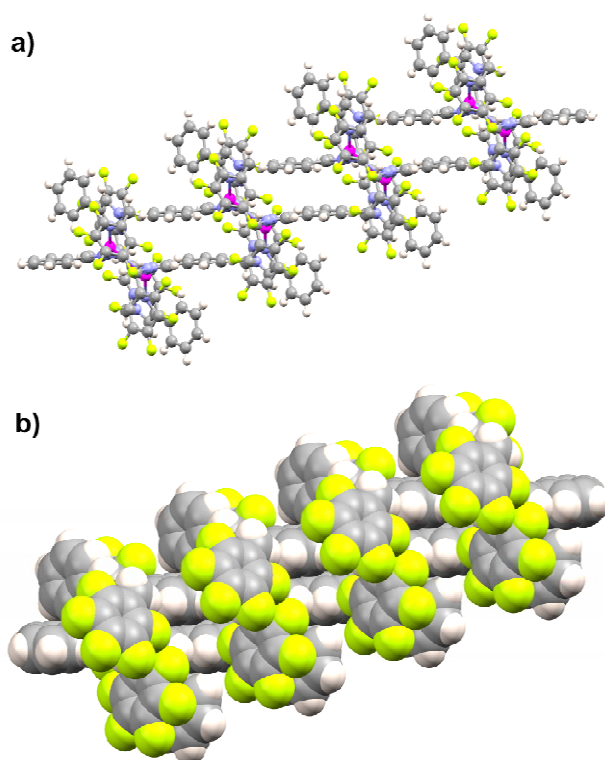


Figure 19. Two views of the extended structure of $[(2b)_2Ag_2](SbF_6)_2$ (**3b**). a) a ball and stick diagram and b) a space filling diagram. The SbF_6^- anions are omitted for clarity.

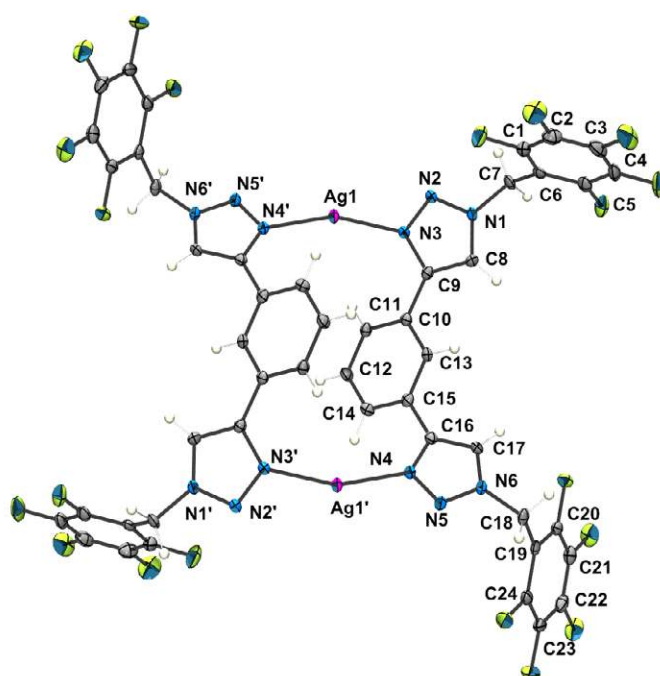


Figure 20. An ORTEP diagram of the $[(3b)_4Ag_2]^{2+}$ cation. The SbF_6^- anions and Et_2O ligands have been omitted for clarity.

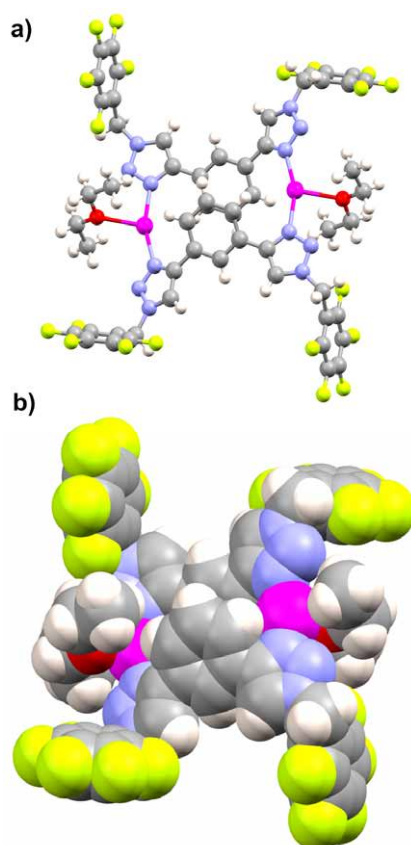


Figure 21. Two views of the complete cationic unit of $[(3b)_2Ag_2](SbF_6)_2$ (**5b**). a) a ball and stick diagram and b) a space filing diagram. The SbF_6^- anions are omitted for clarity.

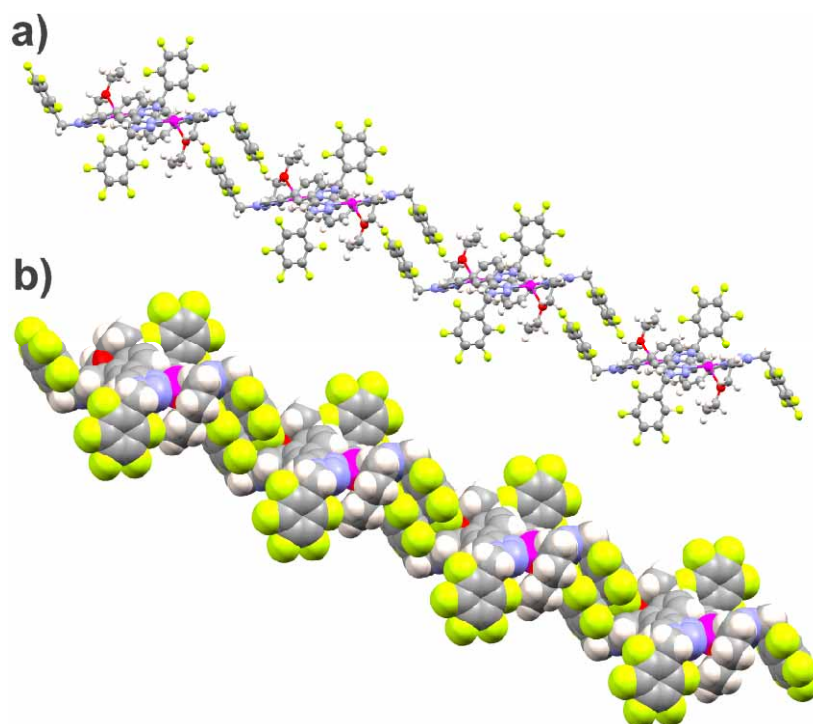


Figure 22. Two views of the extended structure of $[(3b)_2Ag_2](SbF_6)_2$ (**5b**). a) a ball and stick diagram and b) a space filing diagram. The SbF_6^- anions are omitted for clarity.

4.1 X-Ray data collection and refinement for **5b** (acetone).

X-Ray data for **5b** (acetone) was recorded with a Bruker APEX II CCD diffractometer at 89(2) K using Mo K α radiation ($\lambda = 0.71073 \text{ \AA}$). The structure was solved by direct methods using SIR97,¹ with the resulting Fourier maps revealing the location of all non-hydrogen atoms of the core metallomacrocycle unit. Following the location of the core atoms of **5b** (acetone) in the ΔF map there was still residual electron density present near the silver atoms of the structure. This was modelled as coordinated acetone. However, these acetone molecules are badly disordered. Disappointingly, this disorder could not be satisfactorily resolved; as such there is residual electron density around the coordinated acetone molecules within the structure. One of the pentafluorobenzyl groups displayed large thermal parameters potentially due to further disorder, as such it was restrained using ISOR and SIMU commands in SHELXL-97². Weighted full matrix refinement on F^2 was carried out using SHELXL-97² with all non-hydrogen atoms being refined anisotropically, while the disordered acetone molecules were refined isotropically. The hydrogen atoms were included in calculated positions and were refined as riding atoms with individual (or group, if appropriate) isotropic displacement parameters.

The ORTEP³ diagrams have been drawn with 50% probability ellipsoids. Crystal data and collection parameters are given in Table 1.

Table 1 Crystal data and structure refinement for **5b** (acetone).

Identification code	5b (acetone) CCDC 751439
Empirical formula	C ₃₃ H ₂₈ O ₃ F ₁₆ AgSbN ₆
Formula weight	1090.23
Temperature	89(2)
Crystal system	Monoclinic
Space group	P2 ₁ /n
a/Å, b/Å, c/Å	19.902(4), 9.080(2), 23.168(5)
α /°, β /°, γ /°	90, 113.594(1), 90
Volume/Å ³	3836.7(14)
Z	4
ρ_{calc} /mg/mm ³	1.887

m/mm^{-1}	1.336
F(000)	2136
Crystal size	$0.58 \times 0.28 \times 0.07$
Theta range for data collection	1.14 to 24.59°
Index ranges	$-23 \leq h \leq 23, -10 \leq k \leq 10, -27 \leq l \leq 27$
Reflections collected	72868
Independent reflections	6446 [R(int) = 0.062]
Data/restraints/parameters	6446/127/503
Goodness-of-fit on F^2	1.078
Final R indexes [$I > 2\sigma(I)$]	$R_1 = 0.0801, wR_2 = 0.206$
Final R indexes [all data]	$R_1 = 0.0873, wR_2 = 0.2119$
Largest diff. peak/hole	3.089/-1.063

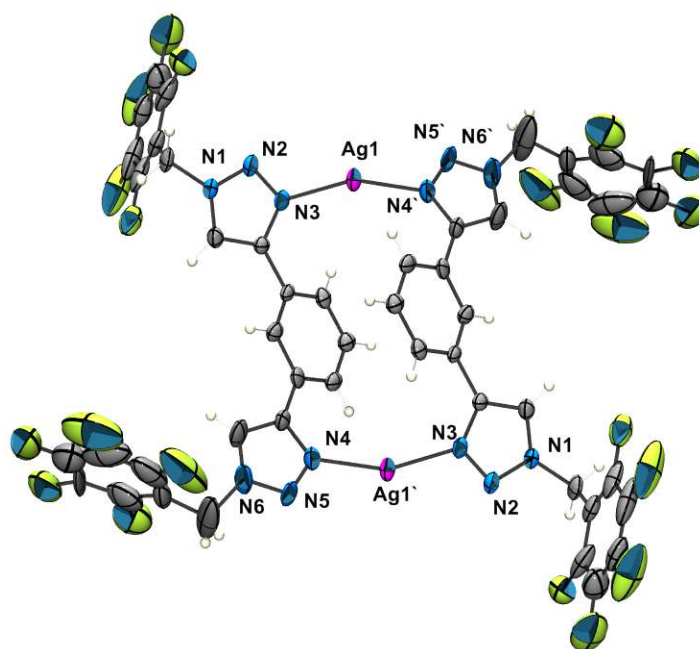


Figure 23. An ORTEP diagram of $[(3b)_4Ag_2]^{2+}$ cation from the of the crystal structure **5b** (acetone). The SbF_6^- anions and acetone ligands have been omitted for clarity.

5. References

1. A. Altomare, M. C. Burla, M. Camalli, G. L. Cascarano, C. Giacovazzo, A. Guagliardi, A. G. G. Moliterni, G. Polidori and R. Spagna, *J. Appl. Crystallogr.*, 1999, **32**, 115-119.
2. G. M. Sheldrick, *Acta Crystallogr., Sect. A: Found. Crystallogr.*, 2008, **A64**, 112-122.
3. L. J. Farrugia, *J. Appl. Crystallogr.*, 1997, **30**, 565.